



ELSEVIER

Physica C 288 (1997) 249–254

PHYSICA C

Morphology and characterization studies of Y doped Bi-2212 single crystals

D. Prabhakaran^{*}, A. Thamizhavel, C. Subramanian*Crystal Growth Centre, Anna University, Madras, 600 025, India*

Received 2 June 1997; revised 12 June 1997; accepted 3 July 1997

Abstract

Superconducting Bi-2212 single crystals of nominal composition $\text{Bi}_{2.2}\text{Sr}_{1.9}\text{CaCu}_2\text{O}_8$, $\text{Bi}_{2.1}\text{Y}_{0.1}\text{Sr}_{1.9}\text{CaCu}_2\text{O}_8$ and $\text{Bi}_{2.2}\text{Sr}_{1.9}\text{Ca}_{0.9}\text{Y}_{0.1}\text{Cu}_2\text{O}_8$ have been grown by flux method using a conical shaped Al_2O_3 crucible. Effect of Y doping on the crystal morphology has been studied. From the X-ray diffraction studies, the cell parameters were calculated. AC susceptibility showed that Y doping gives rise to highest $T_{c,\text{onset}}$ at 92 K and the effect of annealing was also studied. The crystal composition at different places of the crucible and the Al incorporation were studied. The Sr/Ca ratio has been correlated with Y substitution. Chemical etching was also carried out on the grown crystals in order to reveal the nature of twinning and dislocations. © 1997 Elsevier Science B.V.

1. Introduction

High quality single crystals are very much needed for the investigation of intrinsic properties of superconductors. Among the Bi-based high T_c superconductors discovered so far, Bi-2212 phase is the most stable in single crystal form, where as Bi-2223 will decompose into Bi-2212 and Bi-2201 while melting. Different types of crucibles like ZrO_2 , ZrO_2 -stabilized Al_2O_3 and platinum and Al_2O_3 ampoules have been used for the growth of single crystals by flux technique [1–3]. Incorporation of crucible materials into the crystal lattice acts as impurities and alters the superconducting property of the crystal. Several substitutional studies have been carried out to im-

prove the phase purity and transition temperature of Bi-2212 single crystals. Alkaline and Pb doping at different sites increase the T_c by about 10 K [4–6]. On the other hand, 3d metals and rare earth element substitution suppress the T_c value [7–9]. The crystal quality and its properties vary with respect to Sr/Ca ratio and a detailed study of this aspect was carried out by Knizek et al. [10].

Metal insulator transition (MIT) and $\text{Y}_2\text{Cu}_2\text{O}_5$ secondary phase were observed in the Y doped crystals for more than 0.6 mol% substitution [11]. The variation of modulation period and oxygen content with respect to Y doping was studied by Kambe et al. [12]. Twinning is yet another problem in high T_c superconductors and it is commonly observed in YBCO single crystals; it was also observed in Bi-2212 system due to orthorhombic to monoclinic transformation [13]. In the case of Y doped (Ca site)

^{*} Corresponding author. Fax: +91 44 235-2780/2774; e-mail: crystal@sirnetm.ernet.in

Bi-2212 crystals the T_c increases to a maximum of 94 K for 0.2 at% of Y [14,15]. But Hudakova et al. reported that 0.1 at% of Y in the Bi site increases the T_c value by 10 K [16]. Stacking of crystal plates was observed in the Y doped crystals during slow cooling ($0.5^\circ\text{C}/\text{h}$) in flat Al_2O_3 disc crucibles [17]. During fast cooling, at a rate of ($5^\circ\text{C}/\text{h}$), (110) twinning was observed in Y doped single crystals [15]. Annealing of grown crystals in air increases the superconducting property [18–20].

In order to study the effect of Y doping in the Bi-2212 crystals, 0.1 at% of Y was doped in Bi site and Ca site separately. The grown crystals were compared with the undoped crystals and the characterisation studies were carried out using optical microscopy, scanning electron microscopy (SEM), X-ray diffraction (XRD), and AC susceptibility measurements. Composition analysis of grown crystals was done by inductively coupled plasma (ICP) analysis. Etching was done for the grown crystals using different etchants.

2. Experimental

Samples were prepared from powders of Bi_2O_3 , SrCO_3 , CaCO_3 , CuO and Y_2O_3 , of purity greater than 99.9%. The nominal compositions of $\text{Bi}_{2.2}\text{Sr}_{1.9}\text{CaCu}_2\text{O}_8$, $\text{Bi}_{2.1}\text{Y}_{0.1}\text{Sr}_{1.9}\text{CaCu}_2\text{O}_8$ and $\text{Bi}_{2.2}\text{Sr}_{1.9}\text{Ca}_{0.9}\text{Y}_{0.1}\text{Cu}_2\text{O}_8$ (named as B22, B21Y and B22CY respectively) were mixed and ground in an agate mortar for 2–3 h using ethanol. After calcining the mixer at 800°C for 24 h, the powder was used for the crystal growth. Before starting the growth, Al_2O_3 crucibles were recrystallized by preheating them at 1400°C for 5 h in order to minimize the incorporation of foreign particles into the crystal lattice. The synthesized powder of weight 50 g was charged in a crucible of capacity 25 cm^3 ($40\text{ mm height} \times 25\text{ mm diameter}$). The crucible was covered with an alumina lid to prevent contamination and Bi loss. The growth was performed in a vertical muffle furnace using super Kanthal heating rods. The temperature was controlled by a Eurotherm temperature controller (model 818P) with the control accuracy ($\pm 0.1^\circ\text{C}$) using a Pt–Pt/Rh thermocouple. The temperature gradient of the furnace is $0\text{--}1^\circ\text{C}/\text{cm}$ in the axial direction and $1\text{--}2^\circ\text{C}/\text{cm}$ in the radial direction. The

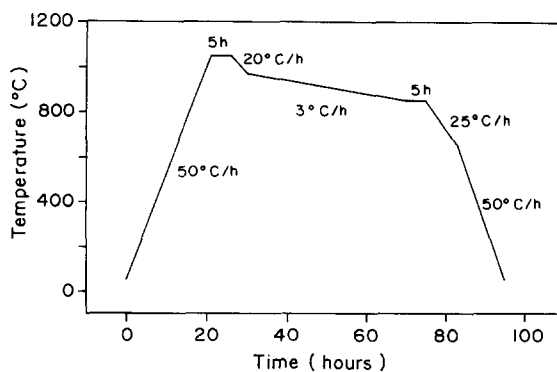


Fig. 1. Schedule of thermal history for the flux growth of Bi-2212 single crystals.

temperature cycle of the growth is given in Fig. 1. After homogenization at 1050°C for 5 h, the melt was cooled to 970°C at a rate of $20^\circ\text{C}/\text{h}$. The growth was carried out at a rate of $3^\circ\text{C}/\text{h}$ from 970 to 850°C . After soaking for 5 h at 850°C the furnace was cooled to 650°C at a rate of $25^\circ\text{C}/\text{h}$ and then to room temperature.

The grown crystals were separated from the crucible by shattering. Using optical microscope (Leica Metallux II) and SEM (Leica Cambridge: Stereoscan 440) surface studies of the separated crystals were carried out. The cell parameter and phase purity of the crystals were performed using a Richt Seifert X-ray diffractometer with $\text{Cu K}\alpha$ (radiation $\lambda = 1.5418\text{ \AA}$). Crystals from different places of the crucible were dissolved in nitric acid and the chemical composition was subsequently quantified by (ICP) analysis. The AC susceptibility studies of as grown and annealed crystals were carried out (Sumotomo, Japan). The etching study was done on the grown crystal using Br_2 -methanol, HCl -acetic acid-methanol (1:4:4) and HNO_3 -acetic acid-methanol (1:4:4) etchants for different periods at room temperature.

3. Results and discussion

3.1. Surface examination

The grown crystals have platelet morphology along the c plane. The B22CY crystals are bigger in size ($10 \times 5 \times 0.01\text{ mm}^3$) when compared to the

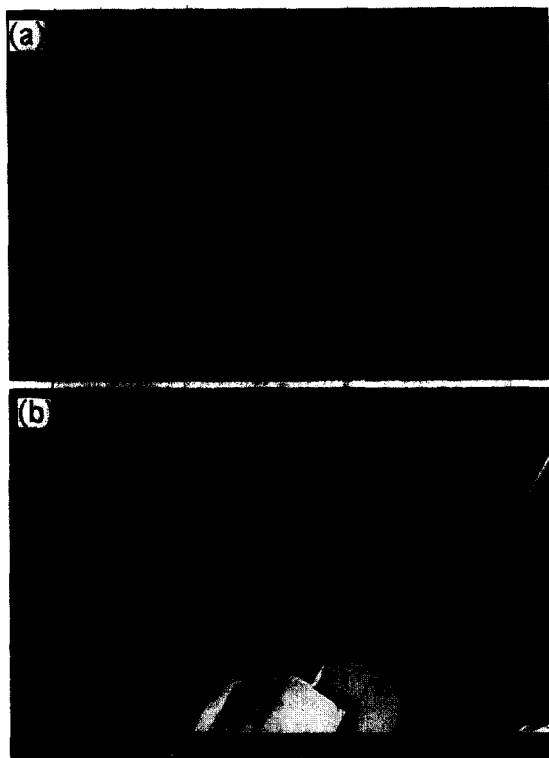


Fig. 2. (a) Scanning electron micrograph of stacking-like morphology of $\text{Bi}_{2.1}\text{Y}_{0.1}\text{Sr}_{1.9}\text{CaCu}_2\text{O}_8$ crystal observed in the middle of the crucible. (b) Magnified view of Fig. 2a.

B22 type crystals. In the case of Y doping (B21Y and B22CY), three types of crystals were identified in the crucible: (i) stacking of plates observed in the middle of the crucible without any flux inclusion (Fig. 2a,b), (ii) crystals with lesser stacking were found along the side walls of the crucible (Fig. 3)



Fig. 3. Optical micrograph of a $\text{Bi}_{2.1}\text{Y}_{0.1}\text{Sr}_{1.9}\text{CaCu}_2\text{O}_8$ crystal found near the wall side of the crucible.



Fig. 4. SEM picture of $\text{Bi}_{2.2}\text{Sr}_{1.9}\text{CaCu}_2\text{O}_8$ single crystal without stacking layers.

and (iii) layered crystals, smaller in size ($5 \times 3 \times 0.01 \text{ mm}^3$) were found on the top surface. In the case of B22 type crystals the maximum size is about $7 \times 5 \times 0.01 \text{ mm}^3$, but there is no stacking order (Fig. 4). Chowdhury et al. have reported that stacking was observed in a flat-bottom crucible with very slow cooling rate (0.5°C/h) [17]. However, in our case the same type of pattern appeared in the crystal grown in a conical shaped crucible even at higher cooling rate (3°C/h). Jayavel et al. have reported that at a cooling rate of 5°C/h , the crystals doped with Y were found to have twinning along (110) plane [15]. But this kind of twinning was not observed in any of our growth runs. The central region of the crucible had plate-like crystals of thickness $10\text{--}30 \mu\text{m}$. Whereas, near the walls the thickness was around $1\text{--}2 \text{ mm}$. But it can be easily cleaved into $40\text{-}\mu\text{m}$ thin layers. Due to flux inclusions the layer growth was disturbed as shown in Fig. 3. This stack of plates was due to Y substitution and the size of the stacking order may vary with growth conditions. In the undoped crystals no such stack or twinning was observed.

3.2. XRD studies

XRD patterns of the as grown crystals are shown in Fig. 5. The cell parameters reveal that all crystals have orthorhombic structure and the values are given in Table 1. Y doping increases the (00 l) peak intensities considerably. With increase of Bi content the b -axis value increases slightly, whereas there is not much change in the value of the a -axis. In the Y doped crystals the value of the c -axis gets reduced

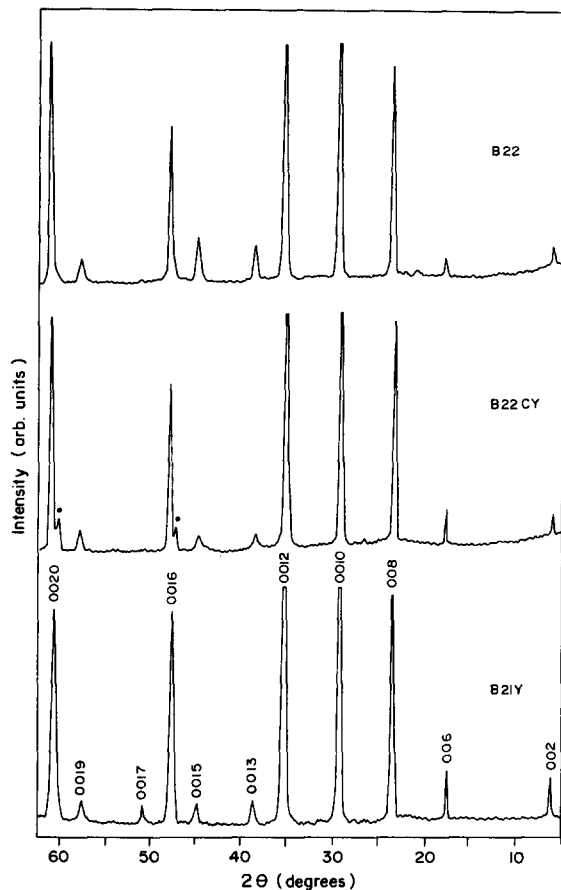


Fig. 5. XRD patterns of $\text{Bi}_{2.2}\text{Sr}_{1.9}\text{CaCu}_2\text{O}_8$ (B22), $\text{Bi}_{2.2}\text{Sr}_{1.9}\text{Ca}_{0.9}\text{Y}_{0.1}\text{Cu}_2\text{O}_8$ (B22CY) and $\text{Bi}_{2.1}\text{Y}_{0.1}\text{Sr}_{1.9}\text{CaCu}_2\text{O}_8$ (B21Y) single crystals.

and this confirms the Y incorporation into the crystal. The c -axis of the B22CY (30.78 Å) is slightly less than that of the B22Y (30.82 Å) crystal and it explains the preference of Y present in the crystal. The cell constants of the crystals found in the middle and the wall portion of the crucible have more or

less the same value. Upon annealing no variation was observed in the Bi-2212 intensity peaks and cell parameter values. The phase purity of the crystal increases with Y doping.

3.3. AC susceptibility studies

The temperature dependent AC susceptibility of the as grown crystals is given in Fig. 6. $T_{c,\text{onset}}$ of all the as grown crystals showed around 80 K, but the $T_{c,\text{zero}}$ of Y doped crystals are 72 K, and 66 K for the undoped (B22) crystals. Transition widths of all the as grown crystals were around 15 K. These low T_c and large ΔT_c values were due to oxygen deficiency in the stoichiometry of the crystal. In order to prevent Bi loss during higher temperature annealing ($> 750^\circ\text{C}$) the crystals were annealed at 650°C . AC susceptibility data of the annealed crystals is given in Fig. 7. The $T_{c,\text{onset}}$ increases about 6–9 K for all the annealed crystals and ΔT_c decreases considerably (about 5 K). The $T_{c,\text{zero}}$ of Y doped crystals (B21Y and B22CY) is 80 K, which is higher (2 K) than in the undoped crystals. Hence, Y incorporation was confirmed by AC susceptibility studies and there is no clear view whether the Y has gone into the Bi or Ca site.

3.4. ICP analysis and etching studies

The chemical composition of the grown crystals was analysed by an ICP method and the values are given in Table 1. Excess amount of Bi (2.2) in the initial composition was taken for the compensation of evaporation loss. Depending upon the Y content in the crystal, the Ca and Sr contents vary and the Sr/Ca ratio increases with respect to Y content. During Y doping, Ca content decreases according to the Y incorporation. But the Bi content variation was

Table 1
Cell parameters, crystal compositions and $T_{c,\text{onset}}$ of annealed crystals

| Nominal composition | Cell parameters (Å) | | | Crystal composition (mol%) (normalised to Cu_2) | | | | | $T_{c,\text{onset}}$ K |
|--|---------------------|------|-------|--|------|------|-----|------|---------------------------|
| | a | b | c | | | | | | |
| | | | | Bi | Sr | Ca | Cu | Y | |
| $\text{Bi}_{2.2}\text{Sr}_{1.9}\text{CaCu}_2\text{O}_8$ (B22) | 5.42 | 5.41 | 30.91 | 2.17 | 1.80 | 0.92 | 2.0 | 0.00 | 89 |
| $\text{Bi}_{2.1}\text{Y}_{0.1}\text{Sr}_{1.9}\text{CaCu}_2\text{O}_8$ (B21Y) | 5.42 | 5.40 | 30.82 | 2.01 | 1.78 | 0.82 | 2.0 | 0.07 | 91 |
| $\text{Bi}_{2.2}\text{Sr}_{1.9}\text{Ca}_{0.9}\text{Y}_{0.1}\text{Cu}_2\text{O}_8$ (B22CY) | 5.41 | 5.38 | 30.78 | 2.17 | 1.88 | 0.74 | 2.0 | 0.14 | 92 |

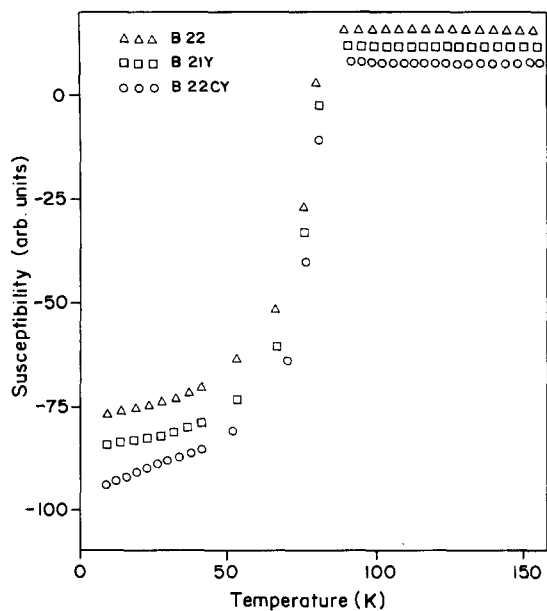


Fig. 6. AC susceptibility data of as grown $\text{Bi}_{2.2}\text{Sr}_{1.9}\text{CaCu}_2\text{O}_8$ (B22), $\text{Bi}_{2.1}\text{Y}_{0.1}\text{Sr}_{1.9}\text{CaCu}_2\text{O}_8$ (B21Y) and $\text{Bi}_{2.2}\text{Sr}_{1.9}\text{Ca}_{0.9}\text{Y}_{0.1}\text{Cu}_2\text{O}_8$ (B22CY) crystals.

very much less. Hence, Y preferably occupies the Ca site rather than Bi site. To confirm the site occupancy more studies are needed, such as NMR analy-

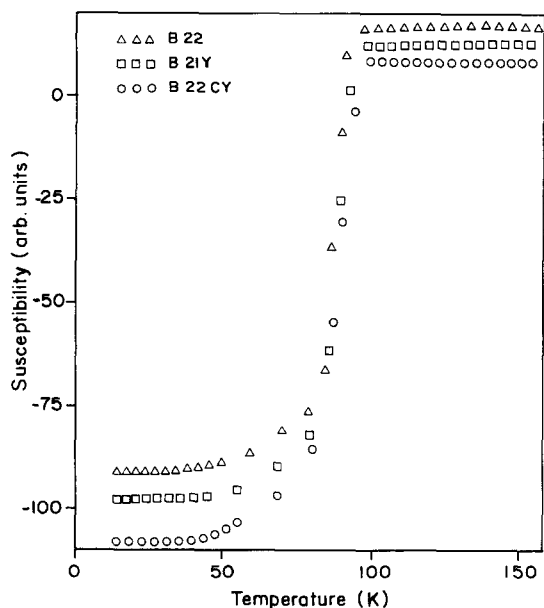


Fig. 7. AC susceptibility data of annealed $\text{Bi}_{2.2}\text{Sr}_{1.9}\text{CaCu}_2\text{O}_8$ (B22), $\text{Bi}_{2.1}\text{Y}_{0.1}\text{Sr}_{1.9}\text{CaCu}_2\text{O}_8$ (B21Y) and $\text{Bi}_{2.2}\text{Sr}_{1.9}\text{Ca}_{0.9}\text{Y}_{0.1}\text{Cu}_2\text{O}_8$ (B22CY) crystals.



Fig. 8. Etch pattern of $\text{Bi}_{2.2}\text{Sr}_{1.9}\text{Ca}_{0.9}\text{Y}_{0.1}\text{Cu}_2\text{O}_8$ crystal (using HNO_3 -acetic acid-methanol mixer for 15 s).

sis. In the wall side crystals, a small amount of Y content variation was observed (0.05 at%) when comparing the middle side crystals. Compositional analysis at the middle of the crucible shows that crucible material (Al) incorporation into the crystal lattice was not found. However, in the wall side crystals trace amounts of Al (0.001 at%) were observed. While considering the annealed crystals the variation in the elemental ratio of the crystal was very small. But the superconducting volume fraction increases, hence in the annealed crystals the only variation is oxygen stoichiometry.

Etching studies for the grown crystals were carried out using 3 types of etchants. The 1% Br_2 -methanol mixer seems to be slowly reactive in nature; only micro twinning was observed in the B22 type crystals and the etching period was about 10–15 minutes. For the HNO_3 -acetic acid-methanol mixer the etching time is very much less (15 s). Stacking layers and screw dislocations were observed in the Y doped crystals as shown in Fig. 8. The HCl mixer seems to be uneven and fast in reaction throughout the surface.

4. Conclusion

Crystals with stack-of-plate morphology were observed in the Y doped Bi-2212 system, while there is no stacking order in the undoped crystals. This growth of stack is an inherent property of dopants like Y and it depends on the growth conditions. The stacking layers are disturbed near the wall side crystals due to inclusions. Due to supersaturation the wall side crystals are thicker in nature. Y doping

decreases the *c*-axis value and it implies that Y occupies the crystal lattice. The Y dopant replaces Ca site rather than Bi site. Annealing increases the T_c value by 6–9 K and superconducting volume fraction. The superconducting volume increases with Y doping and annealing processes. This variation in the annealed crystals is due to variation in the oxygen ratio. Chemical analysis confirms the Y presence in the crystal lattice. Etching studies reveal the layers and screw dislocations.

Acknowledgements

One of the authors (D.P.) gratefully acknowledges the Council of Scientific and Industrial Research, India for the award of Senior Research Fellowship. The authors thank Dr. M.S. Ramachandra Rao, MSRC, Indian Institute of Technology, Madras for extending their characterisation facility. This work is supported by the National Superconductivity Science and Technology Board (NSTB), Department of Science and Technology, Government of India.

References

- [1] L.V. Zhang, J.Z. Liu, M.D. Lan, P. Klavins, R.N. Shetton, *J. Cryst. Growth* 128 (1993) 734.
- [2] A.J.S. Chowdhury, B.M.R. Wanklyn, A.V. Volkozub, J.W. Hodby, *J. Cryst. Growth* 166 (1996) 863.
- [3] M.H. Ionescu, C.C. Sorrell, S.X. Dou, R. Ramer, *J. Superconduct.* 7 (1994) 81.
- [4] S. Wu, J. Schwartz, G.W. Raban Jr., *Physica C* 246 (1995) 297.
- [5] M. Fujiwara, M. Nagae, Y. Kusano, T. Fujii, J. Takada, *Physica C* 274 (1997) 317.
- [6] A. Struk, K. Westerholt, *Physica C* 200 (1992) 215.
- [7] T. Kluge, Y. Koike, A. Fujiwara, M. Kato, T. Noji, Y. Saito, *Phys. Rev. B* 52 (1995) R727.
- [8] U.P.S. Awana, S.K. Agarwal, A.V. Narlikar, M.P. Das, *Phys. Rev. B* 48 (1993) 1211.
- [9] A. Sattar, J.P. Srivastava, S.V. Sharama, T.K. Nath, *Physica C* 266 (1996) 335.
- [10] K. Knizeki, E. Pollert, D. Sedmidubsky, J. Hejtmanek, J. Pracharova, *Physica C* 216 (1993) 211.
- [11] T. Tamegai, K. Koga, K. Suzuki, M. Ichihara, F. Sakai, Y. Iye, *Jpn. J. Appl. Phys.* 28 (1989) L122.
- [12] S. Kambe, K. Okuyama, S. Ohshima, T. Shimada, *Physica C* 250 (1995) 50.
- [13] G. Yang, P. Shang, I.P. Jones, J.S. Abell, C.E. Gough, *Phys. Rev. B* 48 (1993) 16873.
- [14] D.B. Mitzi, L.w. Lombardo, A. Kapitulnik, S.S. Laderman, R.D. Jacowitz, *Phys. Rev. B* 41 (1990) 6564.
- [15] R. Jayavel, A. Thamizhavel, P. Murugakoothan, C. Subramanian, P. Ramasamy, *Physica C* 215 (1993) 429.
- [16] N. Hudakova, P. Samuely, P. Szabo, V. Plechacheki, K. Knizek, D. Sedmidubsky, *Physica C* 246 (1995) 163.
- [17] A.J.S. Chowdhury, N.R. Charnely, F.R. Wondre, A.V. Volkozub, P.A.J. de Groot, B.M.R. Wanklyn, J.W. Hodby, *J. Cryst. Growth* 169 (1996) 405.
- [18] J.-S. Zhu, X.-F. Sun, W.-B. Wu, L.-B. Wang, X.-R. Zhao, G.-E. Zhou, X.-G. Li, Y.-H. Zhang, *Physica C* 256 (1996) 331.
- [19] W.-B. Wu, L.-B. Wang, X.-G. Li, G. Zhou, Y. Qian, Q. Qin, Y.-H. Zhang, *J. Appl. Phys.* 74 (1993) 7388.
- [20] G. Villard, D. Pelloquin, A. Maignan, A. Wahl, *Physica C* 618 (1997) 1.